AD-A066 146 ARMY MISSILE RESEARCH AND DEVELOPMENT COMMAND REDSTO--ETC F/G 17/8
VEHICLE IDENTIFICATION AND TRACKING USING A COHERENT OPTICAL CO--ETC(U)
JAN 79 C R CHRISTENSEN, J UPATNIEKS

UNCLASSIFIED DRDMI-T-79-18 NL

1 OF 1
ADA
066146

END
DATE
FILMED
5 79
DDC

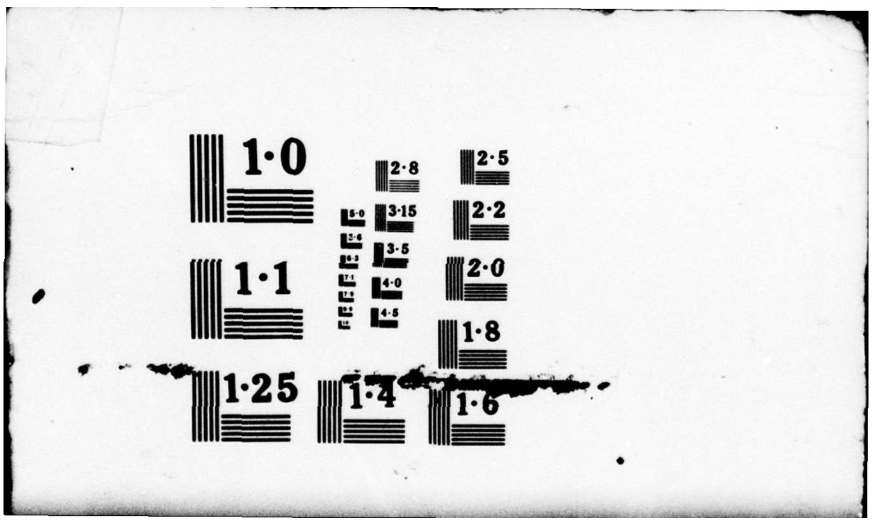
1·0
2·8
2·5
5·0
3·15
2·2
3·5
2·0
1·1
4·0
4·5
1·8
1·25
1·4
1·6

U.S. ARMY MISSILE RESEARCH AND DEVELOPMENT COMMAND

TECHNICAL REPORT T-79-18

VEHICLE IDENTIFICATION AND TRACKING USING A COHERENT OPTICAL CORRELATOR

C. R. Christensen, J. Upatnieks, and B. D. Guenther
Research Directorate
Technology Laboratory

19 January 1979

Redstone Arsenal, Alabama 35809

Approved for public release; distribution unlimited.

DISPOSITION INSTRUCTIONS

DESTROY THIS REPORT WHEN IT IS NO LONGER NEEDED. DO NOT RETURN IT TO THE ORIGINATOR.

DISCLAIMER

THE FINDINGS IN THIS REPORT ARE NOT TO BE CONSTRUED AS AN OFFICIAL DEPARTMENT OF THE ARMY POSITION UNLESS SO DESIGNATED BY OTHER AUTHORIZED DOCUMENTS.

TRADE NAMES

USE OF TRADE NAMES OR MANUFACTURERS IN THIS REPORT DOES NOT CONSTITUTE AN OFFICIAL INDORSEMENT OR APPROVAL OF THE USE OF SUCH COMMERCIAL HARDWARE OR SOFTWARE.

UNCLASSIFIED

SECURITY CLASSIFICATION OF THIS PAGE (When Data Entered)

REPORT DOCUMENTATION PAGE

READ INSTRUCTIONS BEFORE COMPLETING FORM

1. REPORT NUMBER
14 DRDMI-T-79-18

2. GOVT ACCESSION NO.

3. RECIPIENT'S CATALOG NUMBER

4. TITLE (and Subtitle)
6 VEHICLE IDENTIFICATION AND TRACKING USING A COHERENT OPTICAL CORRELATOR,

5. TYPE OF REPORT & PERIOD COVERED
9 Technical Report,

6. PERFORMING ORG. REPORT NUMBER

7. AUTHOR(s)
10 C. R. Christensen, J. Upatnieks B. D. Guenther

8. CONTRACT OR GRANT NUMBER(s)
16

9. PERFORMING ORGANIZATION NAME AND ADDRESS
Commander
US Army Missile Research and Development Command
Attn: DRDMI-TRO
Redstone Arsenal, Alabama 35809

10. PROGRAM ELEMENT, PROJECT, TASK AREA & WORK UNIT NUMBERS
DA 1L161102AH49 17 ØØ
AMCMS 611102.H490011

11. CONTROLLING OFFICE NAME AND ADDRESS
Commander
US Army Missile Research and Development Command
Attn: DRDMI-TI
Redstone Arsenal, Alabama 35809

12. REPORT DATE
11 19 Jan[redacted]79

13. NUMBER OF PAGES
34

14. MONITORING AGENCY NAME & ADDRESS (if different from Controlling Office)
12 34p.

15. SECURITY CLASS. (of this report)
UNCLASSIFIED

15a. DECLASSIFICATION/DOWNGRADING SCHEDULE

16. DISTRIBUTION STATEMENT (of this Report)

Approved for public release; distribution unlimited.

17. DISTRIBUTION STATEMENT (of the abstract entered in Block 20, if different from Report)

18. SUPPLEMENTARY NOTES

19. KEY WORDS (Continue on reverse side if necessary and identify by block number)

Coherent optical correlator
Multiplexed filters
Scale sensitivity
Two-channel correlator
Real-time vehicle tracking

20. ABSTRACT (Continue on reverse side if necessary and identify by block number)

This report describes experiments with a coherent matched filter optical correlator that demonstrates the feasibility of compact correlators identifying vehicles from any perspective and tracking them in real time. The number of required separate filters are greatly reduced with multiplexing schemes. Any sensor with resolution equivalent to that of consumer TV components is adequate to form the correlator input image.

DD FORM 1 JAN 73 1473 EDITION OF 1 NOV 65 IS OBSOLETE

UNCLASSIFIED 393 427

SECURITY CLASSIFICATION OF THIS PAGE (When Data Entered)

79 03 19 017

CONTENTS

I. INTRODUCTION

Coherent optical correlators have been applied to a number of problems of interest to the Army. Successful demonstrations have shown that such correlators could be used for terminal guidance[1,2] aerial reconnaissance film screening [3], assembly line monitoring [4], and character recognition [5].

In most cases emphasis has been placed on the large data handling capacity [6, 7, 8] that can be achieved using large diffraction-limited lenses, liquid gates, and ultra-precise optical systems. While this approach yields impressive results and high estimates for the data-handling capacity, they are not very practical outside a research laboratory. We have explored the opposite approach to coherent optical processing, that of working with minimal image resolution, without liquid gates, and primarily using simple lenses of relatively low quality. The purpose of this approach is to determine if such correlators can be made to operate reliably outside a laboratory environment and in real time; if they can be packaged into small lightweight, rugged assemblies; and if they can still perform useful functions in real-world situations. To date a number of experiments have been performed and the results have been very encouraging.

In this investigation the usefulness of a coherent optical correlator for real-time vehicle recognition and tracking was evaluated. A passenger vehicle and model tank were used as objects to test the correlator. A standard closed-circuit television system was used as the source of the input image which was then entered into the correlator using a noncoherent-to-coherent image converter [9,10].

II. REAL-TIME TRACKING

A. Single Channel Correlator

A diagram of the correlator used in the experiments is shown in Figure 1. In this correlator a monitor displays an image of an outdoor scene from a TV camera. The scene can also be recorded on video tape for future playback. The TV monitor (a consumer Panasonic Model No. CT-911VA color TV receiver) is imaged by L_1 (a 50-mm focal length, f/1.4 lens) onto a liquid crystal light valve [9,10] which generates the coherent input image to the correlator by modulating the polarization of the coherent beam. Mathematically, the processor is used to calculate the cross-correlation r(u,v) between an input f(x,y) and a stored reference h(x,y).

$$r(u,v) = \iint_{-\infty}^{\infty} f(x,y)\, h(u + x, v + y)\, dxdy.$$

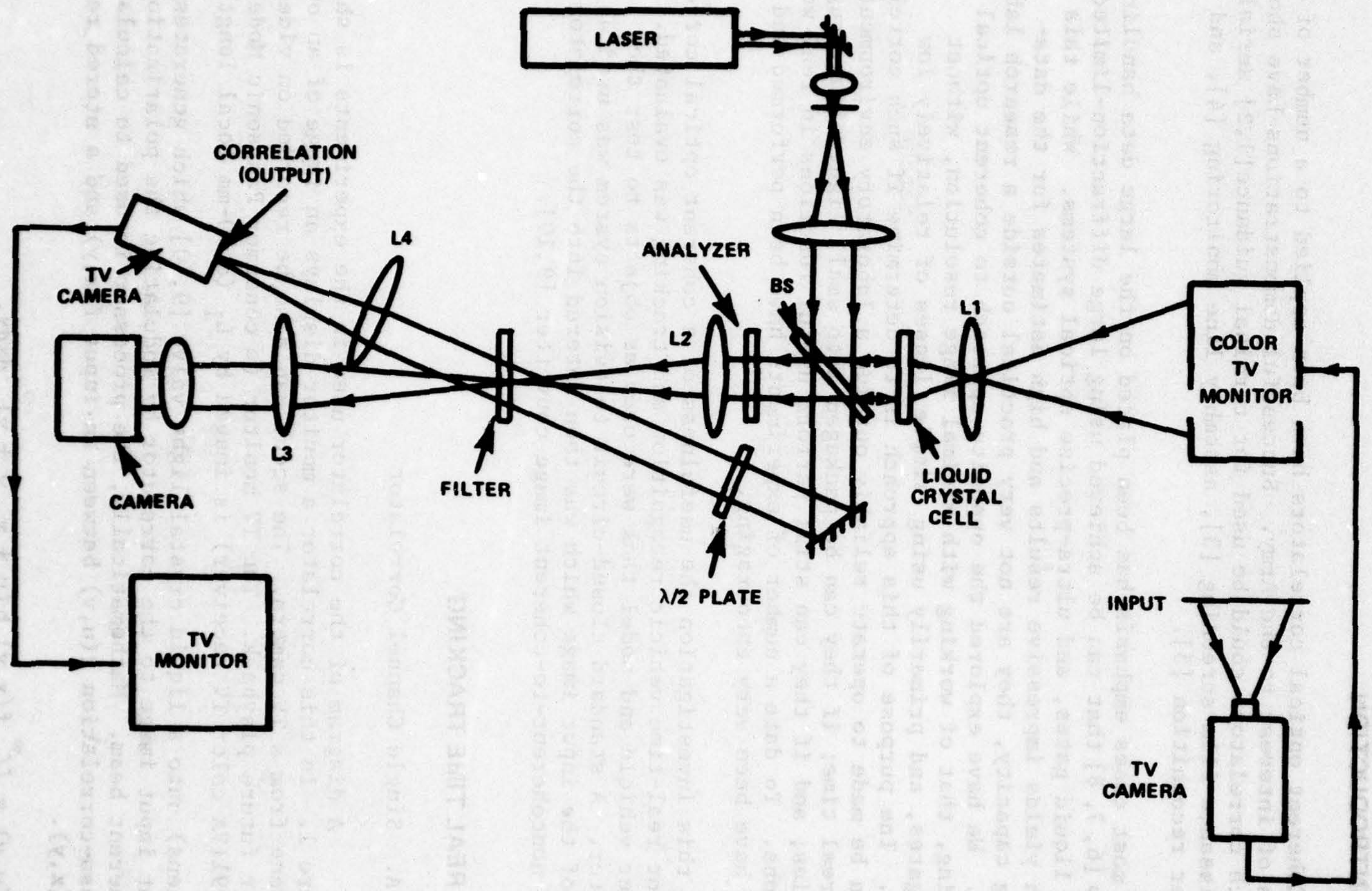

Figure 1. Coherent optical correlator.

To accomplish this, lens L_2 (a 381-mm focal length telescope objective) is used to form a Fourier transform of the reference image, H(p,q). By using a reference beam (Figure 1), H*(p,q) is holographically recorded, where the asterisk (*) denotes the complex conjugate. After recording H*(p,q), the reference beam can be blocked as it will no longer be needed. Lens L_2 is now used to form the Fourier transform of the input scene F(p,q) at the filter position in Figure 1. The holographic recording, called a matched filter, diffracts the signal F(p,q) H*(p,q) along the direction the reference beam had formerly traveled. Lens L_4 collects this light and forms the correlation function

$$r(u,v) = \iint_{-\infty}^{\infty} F(p,q)\, H^*(p,q) \exp\left[-i(pu + qv)\right] dpdq$$

on the light sensitive surface of a second TV camera.

Figure 2a shows the input image used to make the matched filter as displayed on the TV monitor. Figure 2b shows the coherent image from the light value. In recording the matched filter, a mask is placed over the TV monitor to cover all of the scene except the area occupied by the vehicle. The vehicle's height was 24 TV lines, corresponding to twice the Johnson criteria for identification [11]. Figure 2c shows a magnified view (approximately 50X) of the matched filter. The 0 to 50 scale superimposed on the matched filter image corresponds to 1 mm. The range of intensities in the Fourier transform greatly exceeds the dynamic range of the photosensitive material used to record the matched filters (Agfa-Gevaert 10E75 glass plates), allowing us to incorporate bandpass filtering in the matched filter. The spatial frequencies that are passed by the bandpass filter are selected by adjusting the intensity of the reference beam and the exposure used to record the matched filter. In the experiments, the matched filter used operated over the spatial frequency range of 0.38 to 4.6 ℓ/mm, corresponding to the resolution of objects on the TV monitor from 24 TV lines to 2 TV lines in size. Figure 2d shows the matched filter impulse response. As can be seen, only the edges of the vehicle are used in the identification process.

The basic operation of the correlator is shown in Figure 3. The first column shows photographs of the TV monitor input, the second column is the correlation plane as seen by the second TV camera, and the third column displays oscilloscope traces of the TV line scan through the correlation spot. As can be seen in Figure 3, when the vehicle is not present in the scene the correlation spot is absent from the correlation plane.

Figure 4 contains data arranged in the same way as in Figure 3. To record the images for the figures in this report and to record the matched filters of the automobile, it was necessary to stop the video tape and display a single interlace field of a TV frame. When this was done a herringbone pattern appeared on the input image. This pattern was not present when the tape was allowed to play normally on the

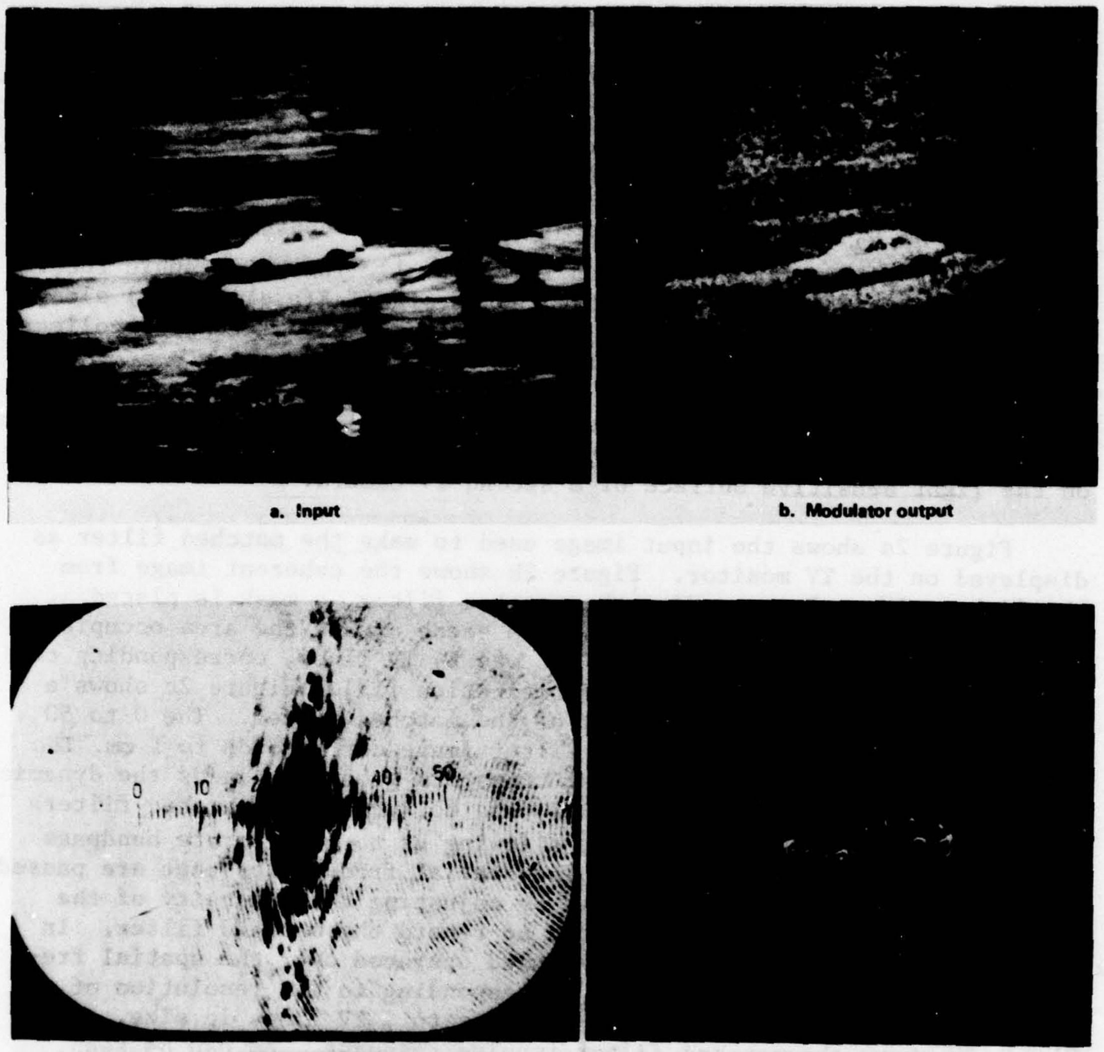

a. Input

b. Modulator output

c. Matched filter

d. Filter reconstruction

Figure 2. Correlator images.

recorder. A comparison of columns one and two of Figure 4 reveals the ability of the correlator to develop tracking signals. As the car moves along the road from the upper right to the lower left of the scene, the correlation spot moves along an equivalent path in the correlation plane. The photographs in the first two rows are reproduced to the same scale; thus the size of the correlation spot in Figure 4 corresponds to the tracking precision of the correlator. The half-width at half-height of the correlation spot is equivalent to a 1.7 TV line displacement of the vehicle in the input scene. The decrease in amplitude of the correlation peak at the edges of the scene is due primarily to image distortions near the edges of the TV monitor used for the correlation input.

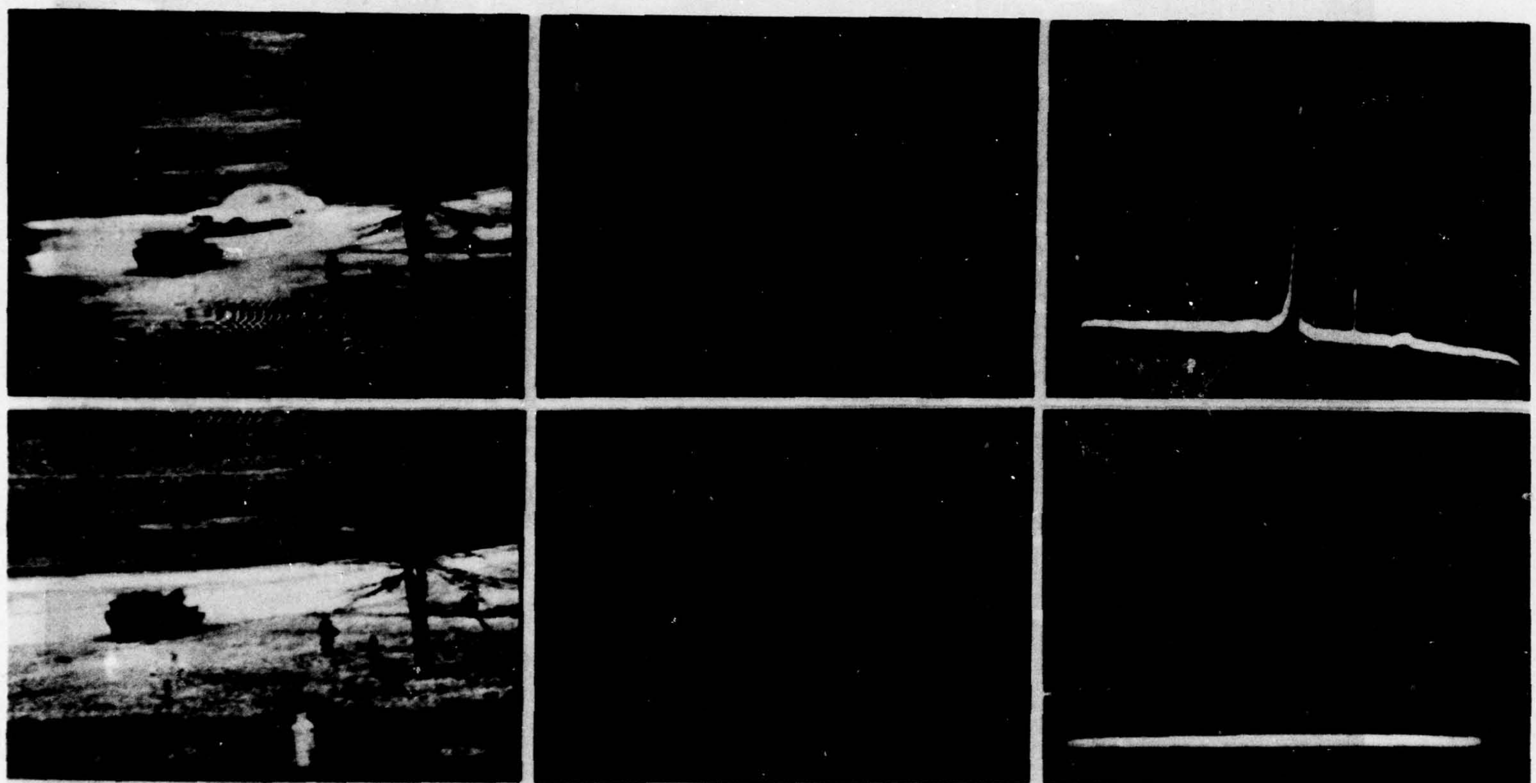

a. Input   b. Correlation plane   c. Line scan

Figure 3. Correlator operation.

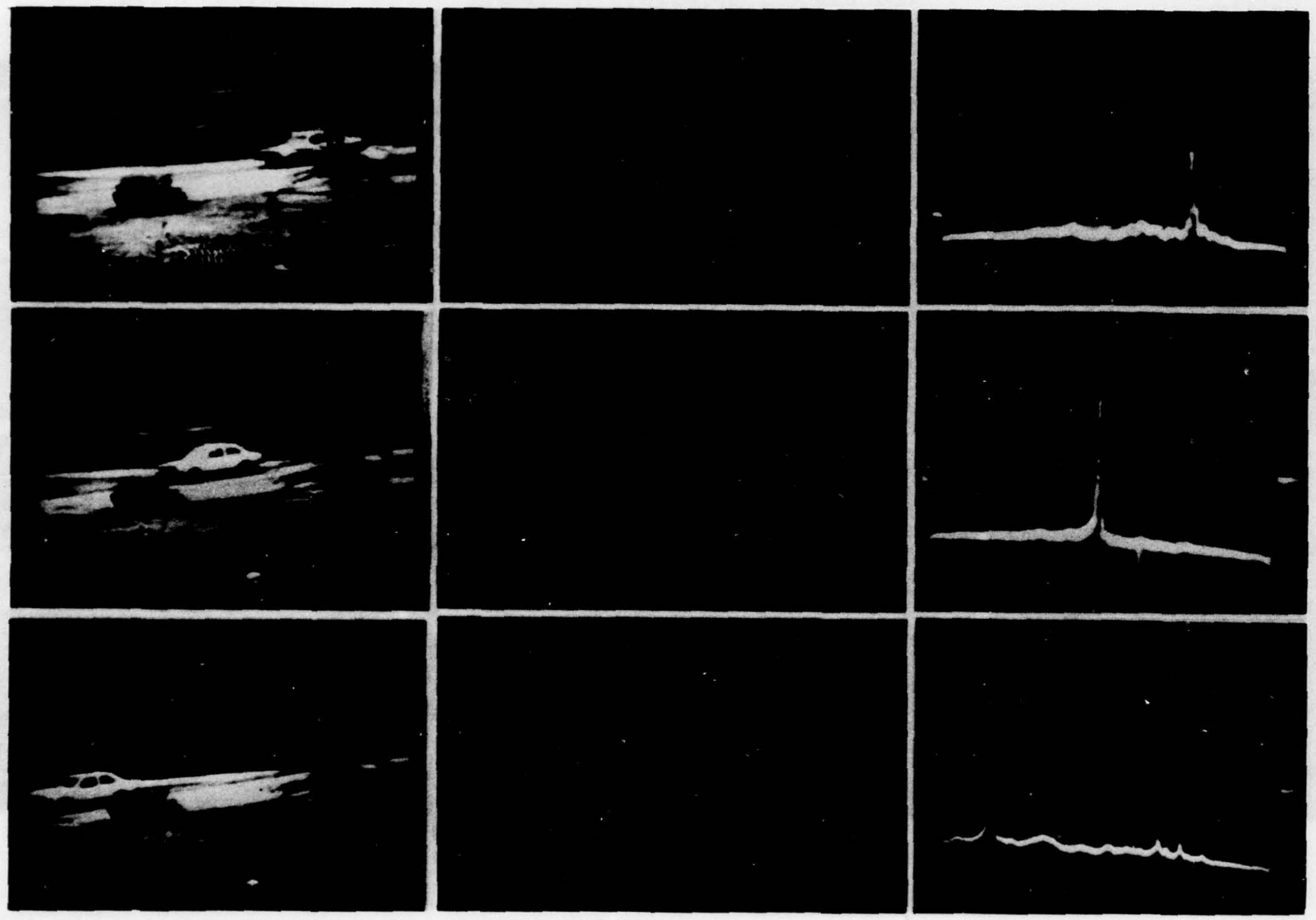

Figure 4. Vehicle tracking with camera in fixed position.

To demonstrate the performance of the optical correlator in a tracking role, the data shown in Figure 5 were obtained. To simulate a tracking operation a video tape was produced containing the image of the vehicle as it moved along a street. The vehicle was manually kept in the center of the scene to simulate the operation of an automatic tracker. Individual frames from the video tape are shown in Figure 5. The matched filter used in the processor is shown in Figure 2 and corresponds approximately to the second frame from the left in the top row of images in Figure 5. The video tape was input to the processor and oscilloscope traces of TV scan lines through the correlation spot were recorded and are shown in Figure 5. The correlation peak amplitude increases and then decreases as the vehicle moves toward and then away from the filter recording position. To display the relative output signal-to-noise ratios, the correlator output was adjusted for each scan line shown to maintain the same approximate peak height. Over the first seven frames of the sequence, the correlation peak amplitude remains well above that of any false peaks, as can be seen by examining the TV scan line presentations in Figure 5. During this sequence the size of the vehicle image changed by 45%, and there was a noticeable change in perspective. In the last two frames of Figure 5, excessive change in the size and perspective of the vehicle results in the loss of a unique correlation spot. Images of the correlation plane for the last four frames of the sequence are shown in Figure 5 and illustrate that the unique correlation peak is decaying into a cluster of small peaks distributed over the vehicle image area. Over most of the tracking demonstration shown in Figure 5, a simple threshold algorithm and automatic gain control are all that is required to use the correlator for tracking. The correlator could still be used for tracking when the correlation peak begins to break up by implementing a more complicated algorithm. However, a simpler solution exists and will be discussed in Paragraph II.B.

B. Dual Filter Processor

Figure 5 showed that a distinct correlation peak is visible over a limited range of vehicle positions. As the vehicle moves away from the filter recording position, the scale and aspect angle changes and the correlation peak amplitude decreases and eventually the single correlation peak disappears. The range over which correlation can be achieved can be increased by recording a number of matched filters corresponding to several vehicle positions. Each filter would be stored at a different spatial location in the filter plane. The filters can be used simultaneously so that they constitute a multiple parallel channel correlator. Because only the filter that correlates with the input image is of interest, there is no need to illuminate all the filters simultaneously. In fact, engineering design problems associated with correlator power requirements, detector sensitivity, and noise thresholds resulting from scattered light indicate that a sequentially addressed filter memory bank should be used. With existing off-the-shelf components, a correlator can be designed with a memory bank containing 25 sequentially addressed filters [12].

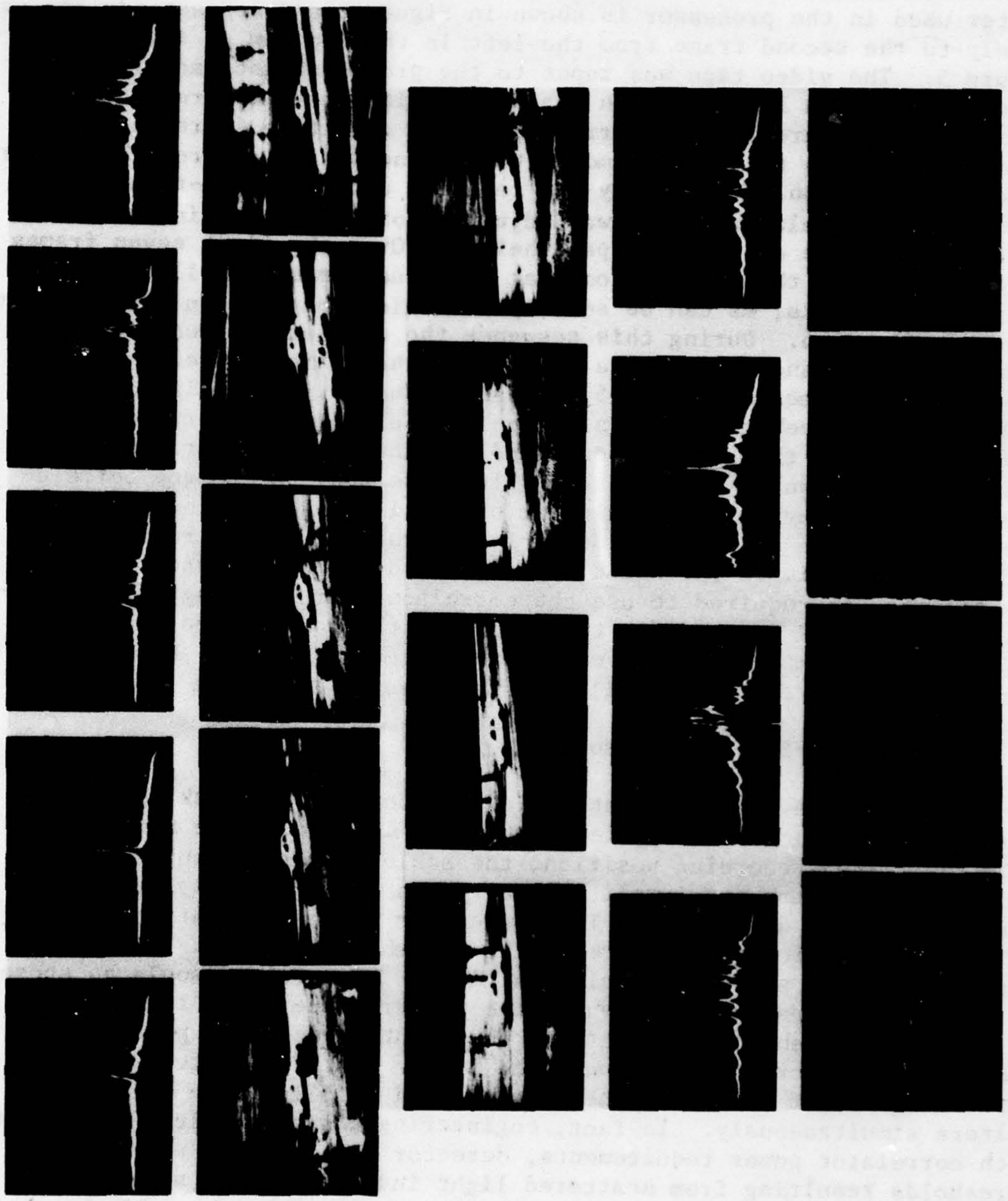

Figure 5. Real-time vehicle tracking with the camera following the vehicle.

To demonstrate the principle, a two-channel parallel processor was assembled (Figure 6). A laser beam collimated by lens L_2 is reflected by mirrors M_1 and M_2 so that the beams overlap at the liquid crystal cell. Each beam forms a separate Fourier transform at the matched filter plane. Mirrors M_4 and M_5 reflect the reference beam used during the filter recording to the Fourier transform plane. Two mirrors M_4 and M_5, rather than one, are required to insure that the same beam from M_1 or M_2 overlap the corresponding Fourier transform at the Fourier transform plane.

Construction of the two filters is accomplished by introducing reference image No. 1 with mirror M_2 blocked, making an exposure and then introducing reference image No. 2 with mirror M_1 blocked and making a second exposure. Once the matched filters are made, mirrors M_4 and M_5 are blocked and the reference beam is no longer used. Correlation spots are detected by a TV camera and can be displayed on a monitor.

The results obtained using the two-channel parallel processor with the same video input as was used in Figure 5 are shown in Figure 7. A matched filter was made of the vehicle at each of the two views noted in the figure. As the vehicle moves from right to left, starting at the upper right hand corner of Figure 7, the correlation signal is best first with filter No. 1 and then with filter No. 2. The two-channel correlator enables us to obtain a useable tracking signal over the entire distance the vehicle was tracked by the TV camera.

III. VEHICLE RECOGNITION

While the recognition of a vehicle is not a problem if the correlation is performed under the same conditions for which the correlator filter was made, the correlation peak becomes smaller if the perspective and illumination angle of the vehicle are changed. To recognize a vehicle from all perspectives and a variety of illumination conditions, a number of filters must be constructed and stored in the correlator. Two objectives of this investigation were to determine the sensitivity of the matched filter to changes in viewing angle, and the sensitivity to changes in illumination angle. A model vehicle was used as the object and the tests were performed in an idealized situation with the model illuminated against a dark background. This, of course, does not represent a real-world situation but it does provide a set of controlled measurements. Combining this controlled data with real-world experiments such as those described in the previous section will provide a realistic appraisal of the performance capabilities of the optical processor.

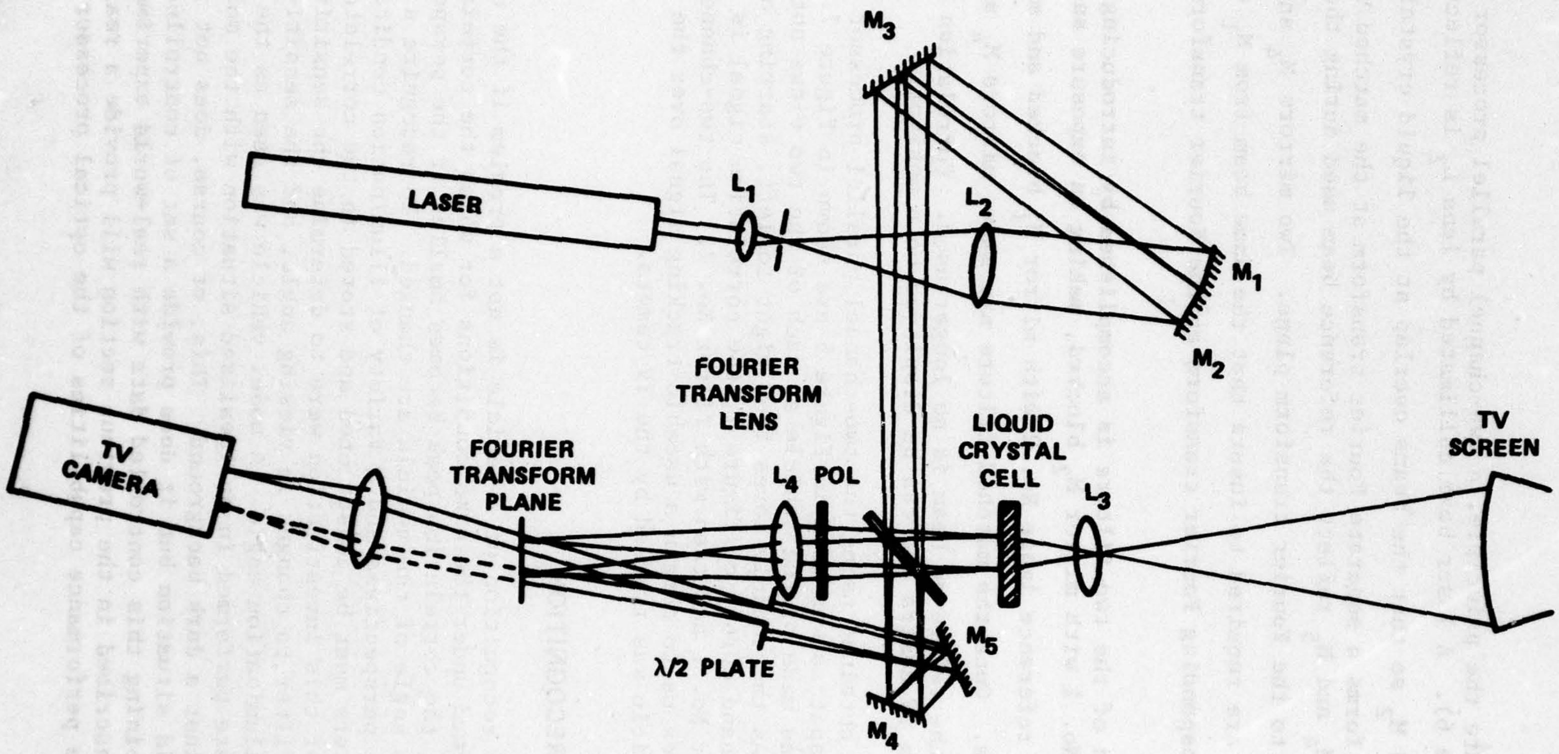

Figure 6. Two-channel coherent optical correlator with a single input image and two filters.

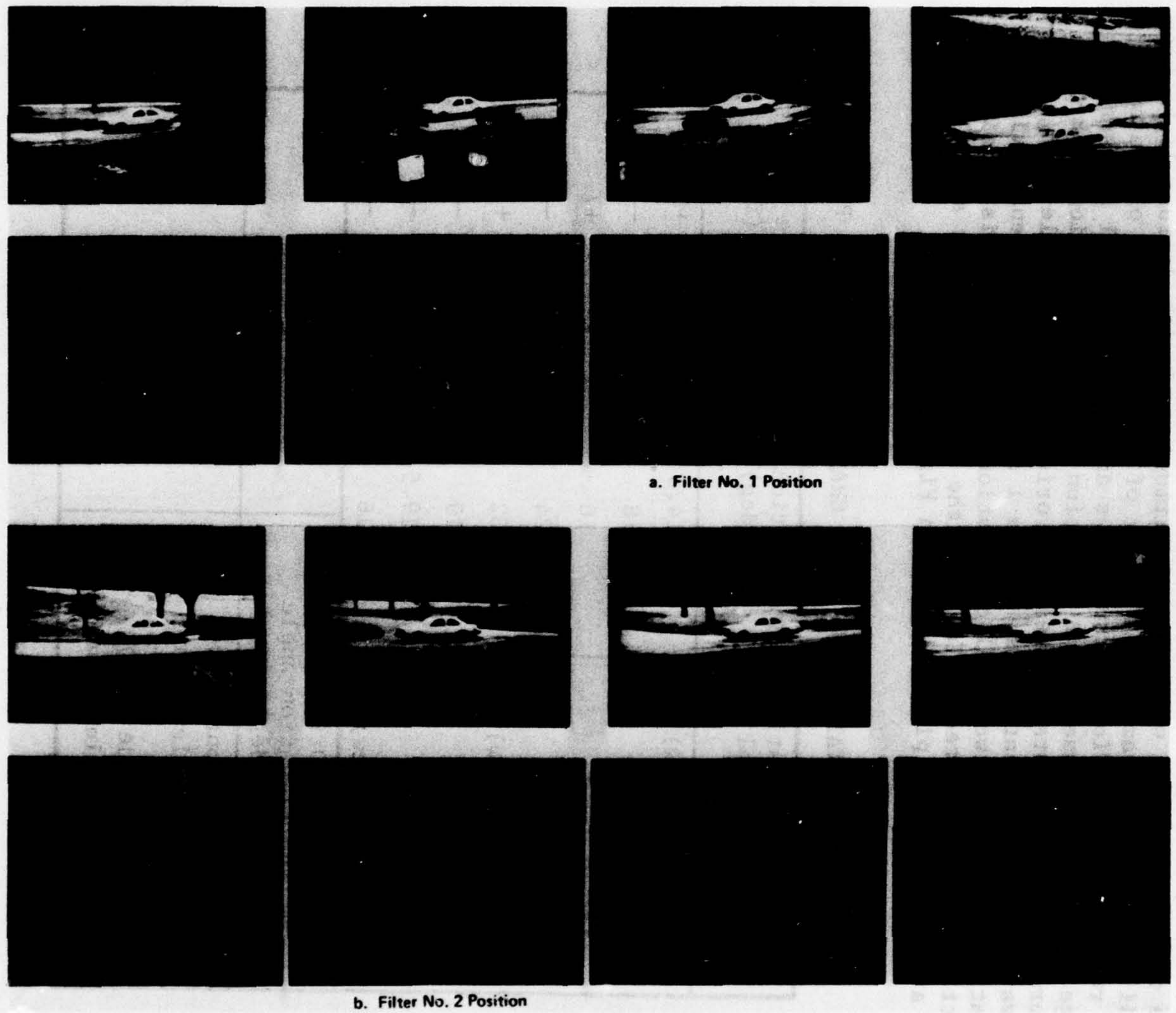

Figure 7. Real-time vehicle tracking using a two-channel correlator.

A. Scale and Perspective Sensitivity of a Single Matched Filter

Experiments were conducted with the optical processor shown in Figure 1 to determine the number of filters needed to recognize a vehicle model from various perspectives both horizontally and vertically. The sensitivity of the filters to scale change was also measured. The TV camera input (Figure 1) viewed the model from various angles. Except where noted, the model was uniformly illuminated with diffuse light from the direction of the camera. A number of matched filters of the model were recorded from various perspectives and the rotational and scale change required to cause a 3-dB reduction of the correlation peak were measured. Table 1 lists the measured orientation and scale changes for various model orientations. Table 1 also lists the sensitivity to elevation change for two model orientations. To aid in visualizing the orientation ranges listed in Table 1, the data for a front and side view are presented in pictoral form in Figure 8.

TABLE 1. ORIENTATION AND SCALE CHANGE BETWEEN 3-dB POINTS

Angular Orientation of Tank Model (deg)	Orientation Range (deg)	Scale Range (%)
0 (Front View)	14.5	±8
22.5	18	—
45	16	±7
67.5	24	—
90 (Side View)	32	±7
112.5	19	—
135	19.5	—
180 (Rear View)	16	—

Angular Orientation and Elevation Angle (deg)	Elevation Range (deg)
0 (Front View), 0 Elevation	~20
90 (Side View), 6 Elevation	29

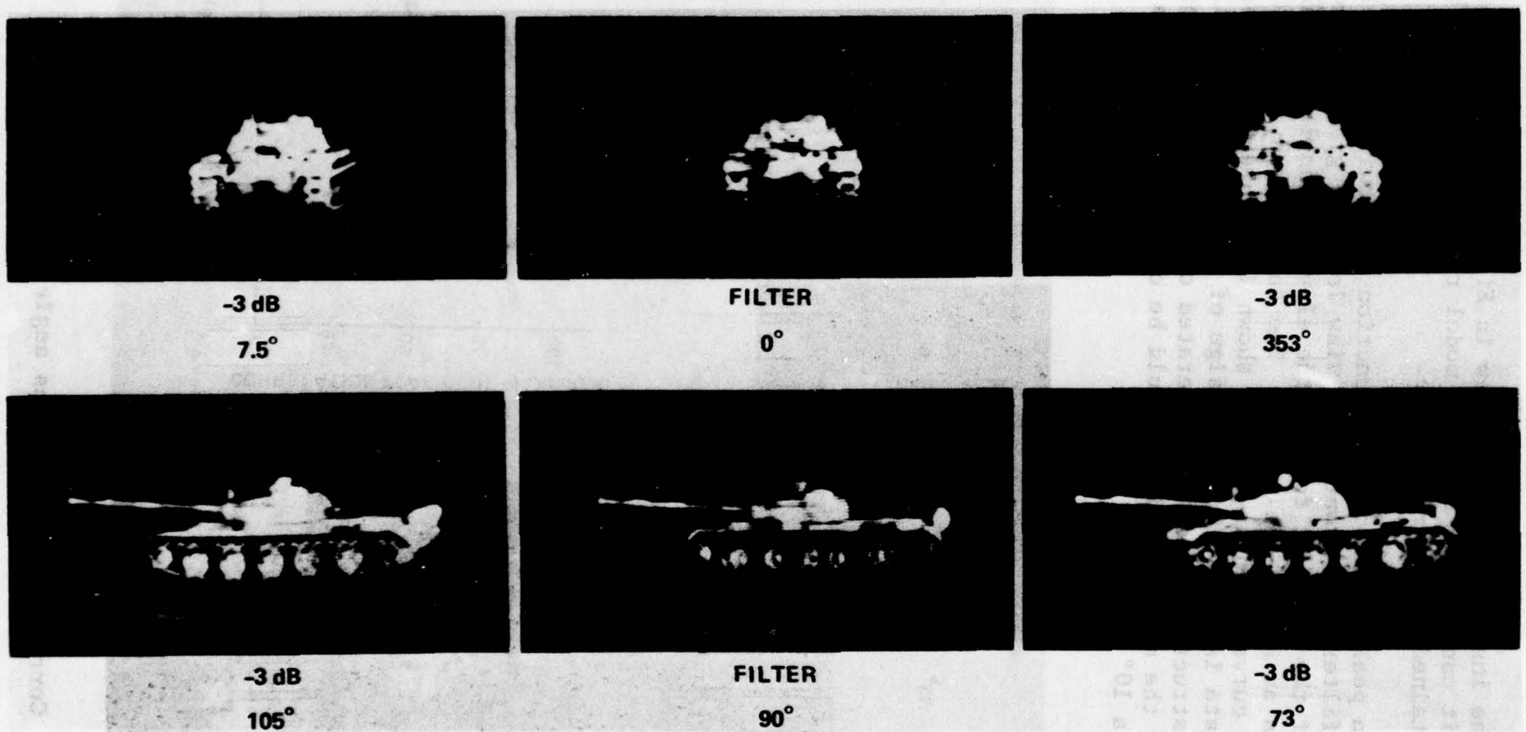

Figure 8. Orientation sensitivity of a single filter.

By comparing the images for a side view in Figure 8 with the images shown in Figure 5, it can be seen that the model results are compatible with the results obtained with a real scene.

The correlation peak amplitude as a function of viewing angle elevation for a matched filter of a front model view is shown graphically in Figure 9. Images of the model at four of the elevation angles are also shown in Figure 9 as an aid to the reader. The data listed in Table 1 were extracted from curves such as the one shown in Figure 9. One use of these types of data is to aid in the design of optimum matched filters. For example, to construct a filter that operated over the maximum spread in elevation angle, the matched filter should be constructed using a reference image at a 10° elevation angle.

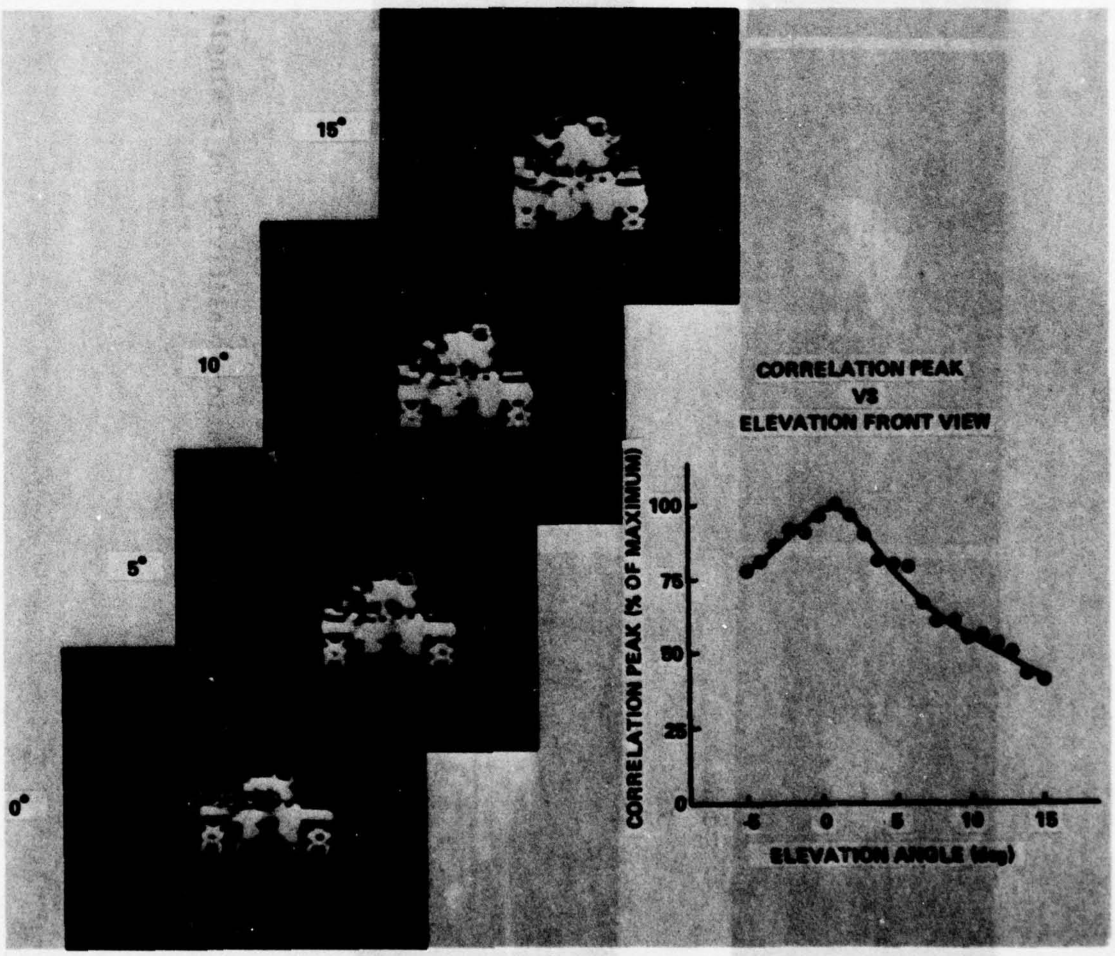

Figure 9. Correlation peak versus angle of elevation.

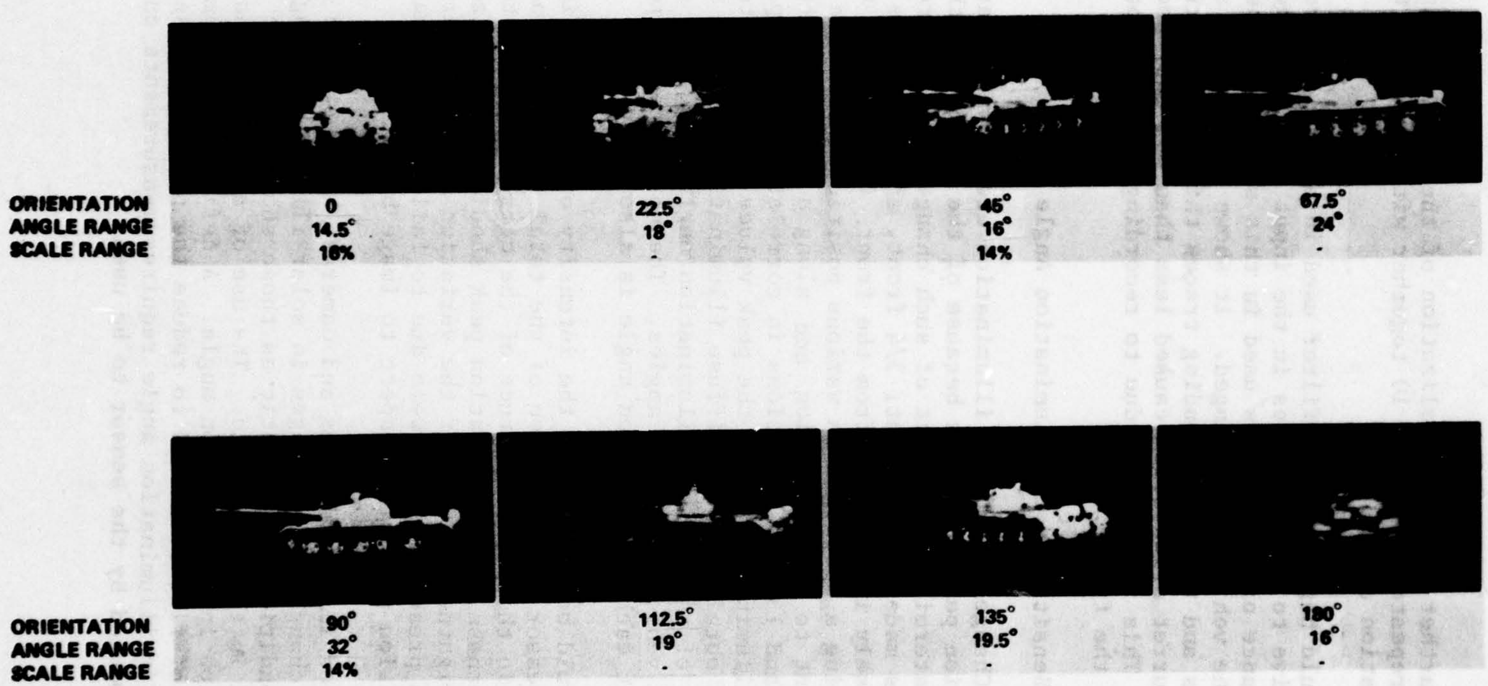

Figure 10. Orientation and scale sensitivity of tank model for various perspectives (range between 3-dB points).

As a further aid in visualization of the data, the information in Table 1 is repeated in Figure 10 together with images of the model at each orientation angle.

One would hope that any filter used in an optical processor would be insensitive to minor changes in the input images. Figure 11 shows the performance of the filters used in this study when the turret orientation of the vehicle was changed. It shows the vehicle and turret orientations and the corresponding traces through the correlation peak. Change in turret orientation caused less than 40% decrease in correlation peak. This is probably due to recording only low spatial frequencies on the filter.

B. Sensitivity to Illumination Angle

Changes in object illumination are known to cause variations in correlation peak amplitude because of the changes in the object appearance. To determine the effect of such changes, tests were performed with filters made of the front, 3/4 front, and side views of the tank model diffusely illuminated from the front. Correlations were then measured using a spotlight in various positions above the tank model along a front to rear direction and along a right to left direction. Figures 12 and 13 show variations in correlation peak amplitude with spotlight illumination, with the peak values normalized to the correlation peak obtained using diffuse illumination. To aid in visualizing the effects of the various illumination angles Figure 14 shows the appearance of the vehicle at three angles. The normalized correlation peak amplitude at each illumination angle is also shown.

It should be noted that the intensity of coherent light available in the processor is a function of the total image brightness. To remove variations in the peak amplitude of the correlation due to variation in image brightness, the correlation peak should be normalized with respect to image brightness. Some of the variation seen in Figures 12 and 13 and in data presented later were due to failure to adequately normalize the correlation peak with respect to image brightness.

Infrared imaging systems and cameras should produce imagery whose appearance changes with changes in solar illumination angle. However, lighting conditions as dramatic as those shown in Figure 14 would not be expected in the real-world. The use of an active sensor would remove the variation in illumination angle. A definitive statement concerning the number of filters needed to reduce the processor's sensitivity to variations in illumination angle requires measurements on real-world imagery produced by the sensor to be used.

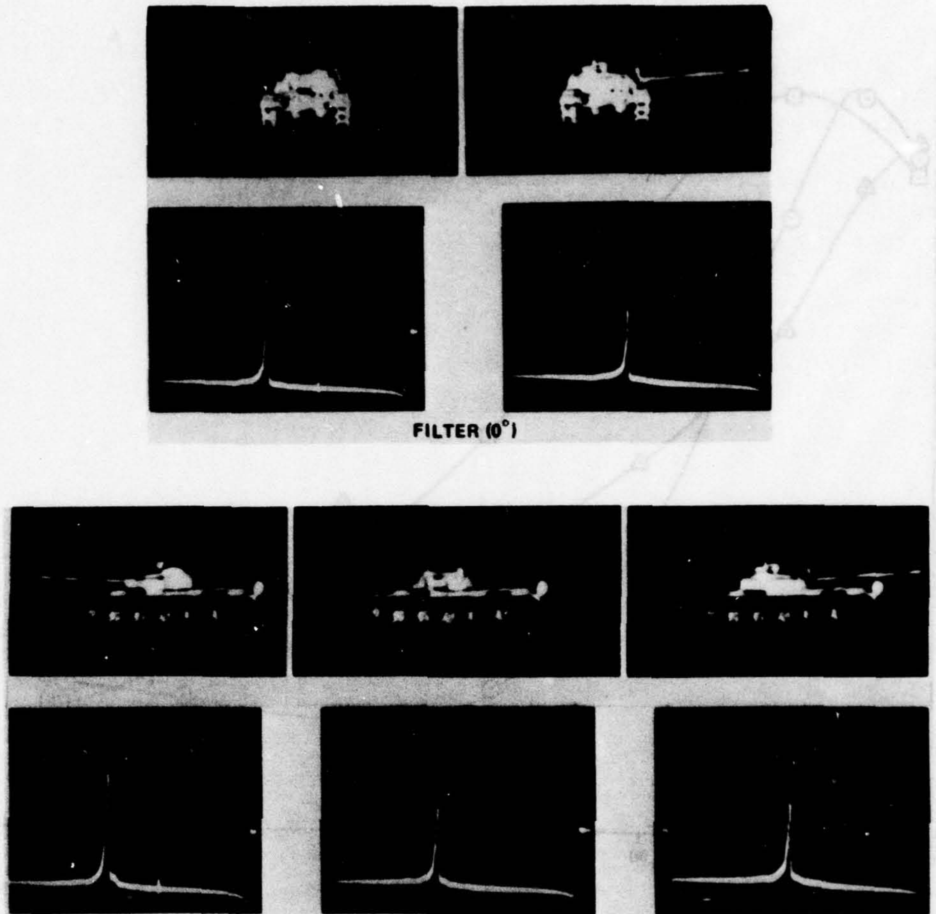

Figure 11. Correlation peak versus turret orientation.

C. Multiplexed Filters

An increase in the angular range over which a matched filter will operate will reduce the number of matched filters that must be stored in the processor.

In order to extend the range of rotation over which a single filter could correlate, the concept of filter multiplexing was tested [6]. Filter multiplexing is accomplished by recording several matched filters at the same spatial location in the Fourier transform plane, each of a different perspective of the vehicle. Since only the vehicle recognition and location is required, the correlation peaks of all superimposed filters can coincide in the output plane. By proper choice of exposure

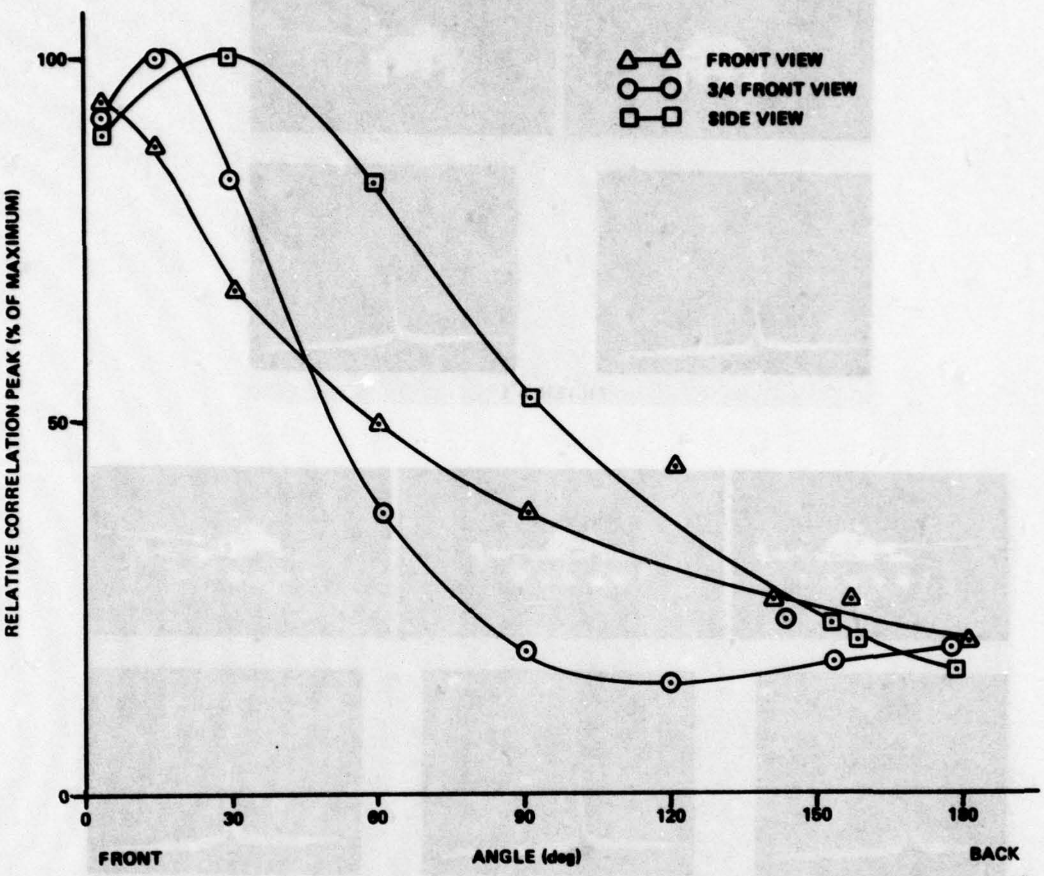

Figure 12. Correlation peak versus illumination angle (front to rear).

lengths and changes in vehicle perspective, a filter can be constructed that can recognize a vehicle over a large change in perspective.

Figure 15 shows the results of an experiment using eight superimposed filters, each made at a different vehicle perspective. A polar plot of the relative correlation peak amplitude is plotted in the center of Figure 15 for a single filter and the eight-fold multiplexed filter. Arrows on the graph indicate the angular orientation of the model vehicle used in recording the eight superimposed filters. The single matched filter produced a correlation peak whose amplitude remained above 40% of its maximum over a 50° angular change. The eight-fold multiplexed filter demonstrated similar performance over 360°. Images of the vehicle are displayed in Figure 15 to aid in visualization.

Figure 16 shows a similar plot with four superimposed filters. The tank can be recognized from all horizontal positions with this filter

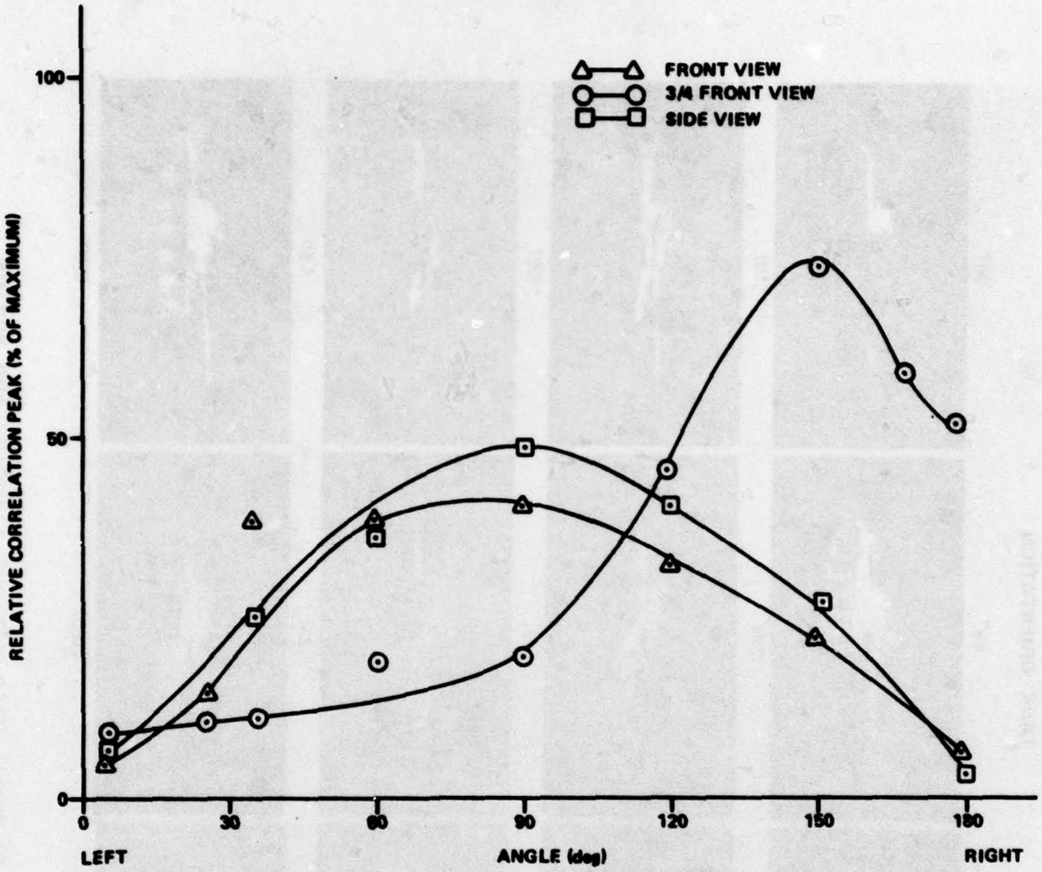

Figure 13. Correlation peak versus illumination angle (side to side).

too, but the correlation peak dips below the 40% level at several spots. Choice of different recording positions and adjustment of exposure level of each filter should make the response curve much more uniform.

A similar test was performed with angle-of-view change in elevation. The response curve of a single filter and four superimposed filters is shown in Figure 17 along with photographs of the tank. In this figure the single filter covers a 29° elevation range while the multiplexed filter covers a 55° elevation range. The multiplexed filter response uniformity can be improved by adjustments in recording positions and in exposure lengths of individual filters.

The question arises as to whether multiplexing destroys the filter's capability to discriminate between various objects. A simple test was performed in which the ability of a matched filter to recognize the

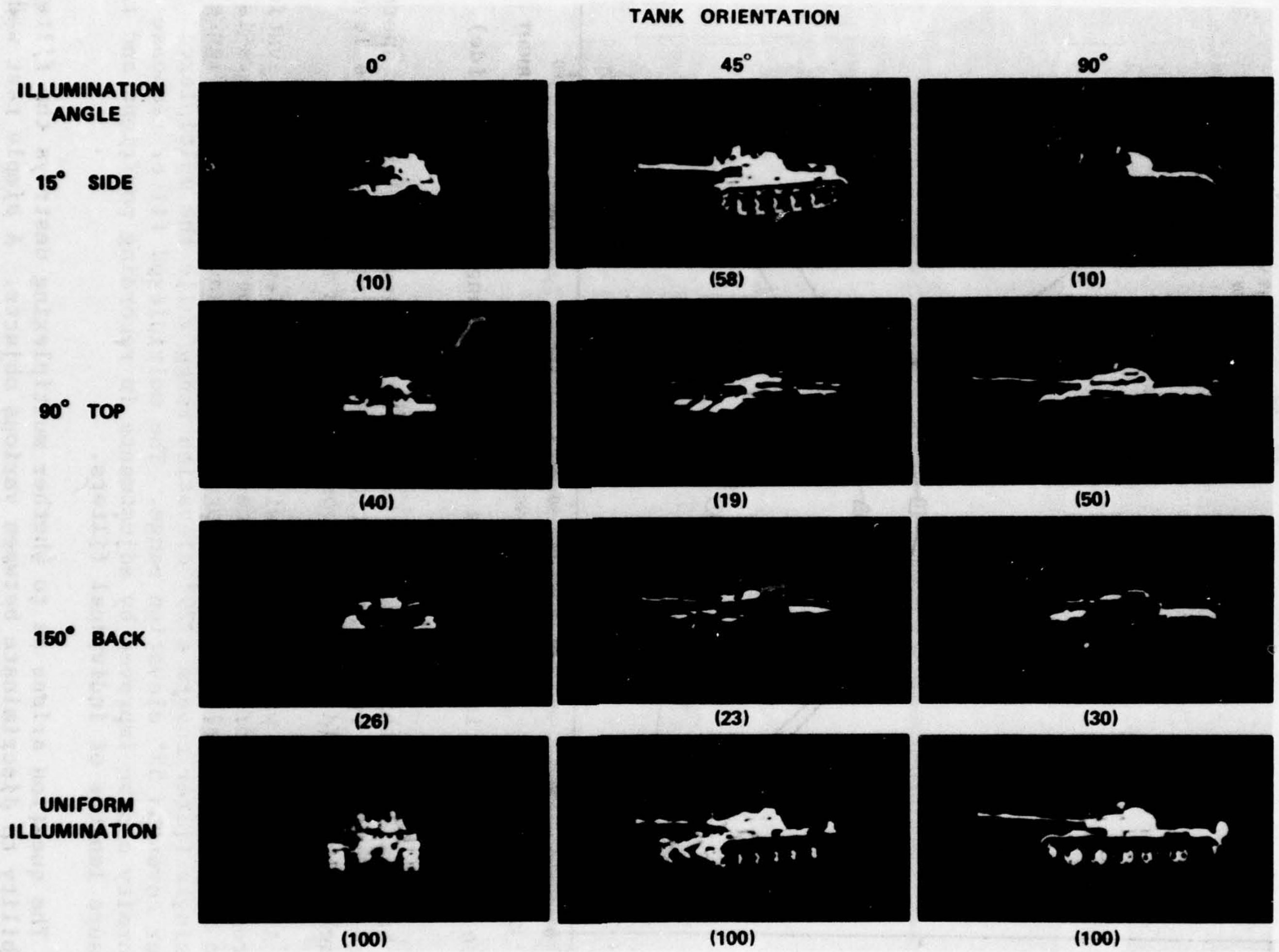

Figure 14. Appearance of model with various illumination angles (normalized correlation peak amplitude).

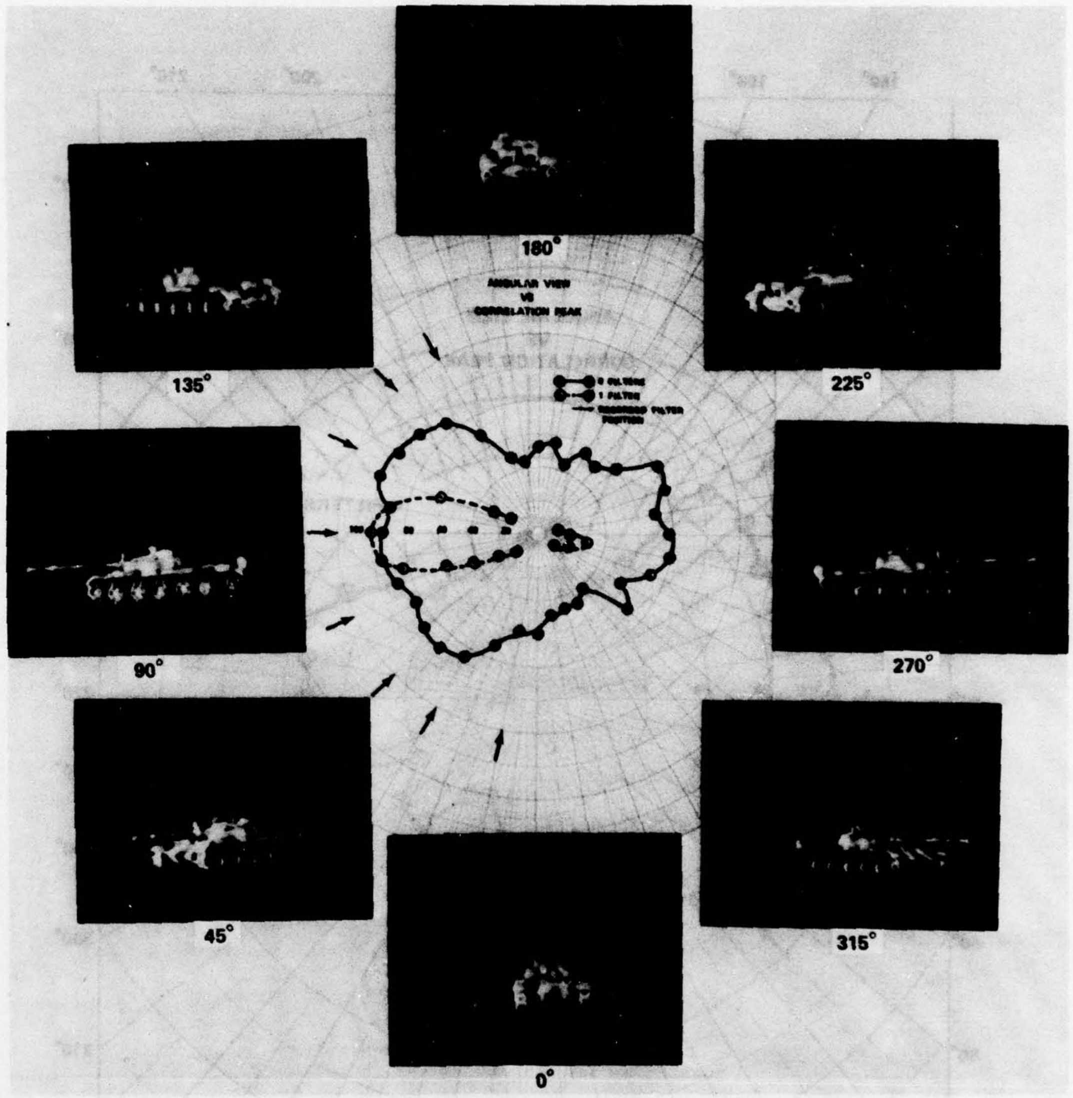

Figure 15. Angular view versus correlation peak of single and eight multiplexed filters.

reference model was compared to the ability of the filter to discriminate against a different model. The results of this test are shown in Figure 18.

In Figure 18 we have recorded a single TV scan line through the correlation peak for the case when the input image was Model A and when the input image was Model B. The matched filters used were constructed using Model A as the reference input. The maximum peak amplitude for

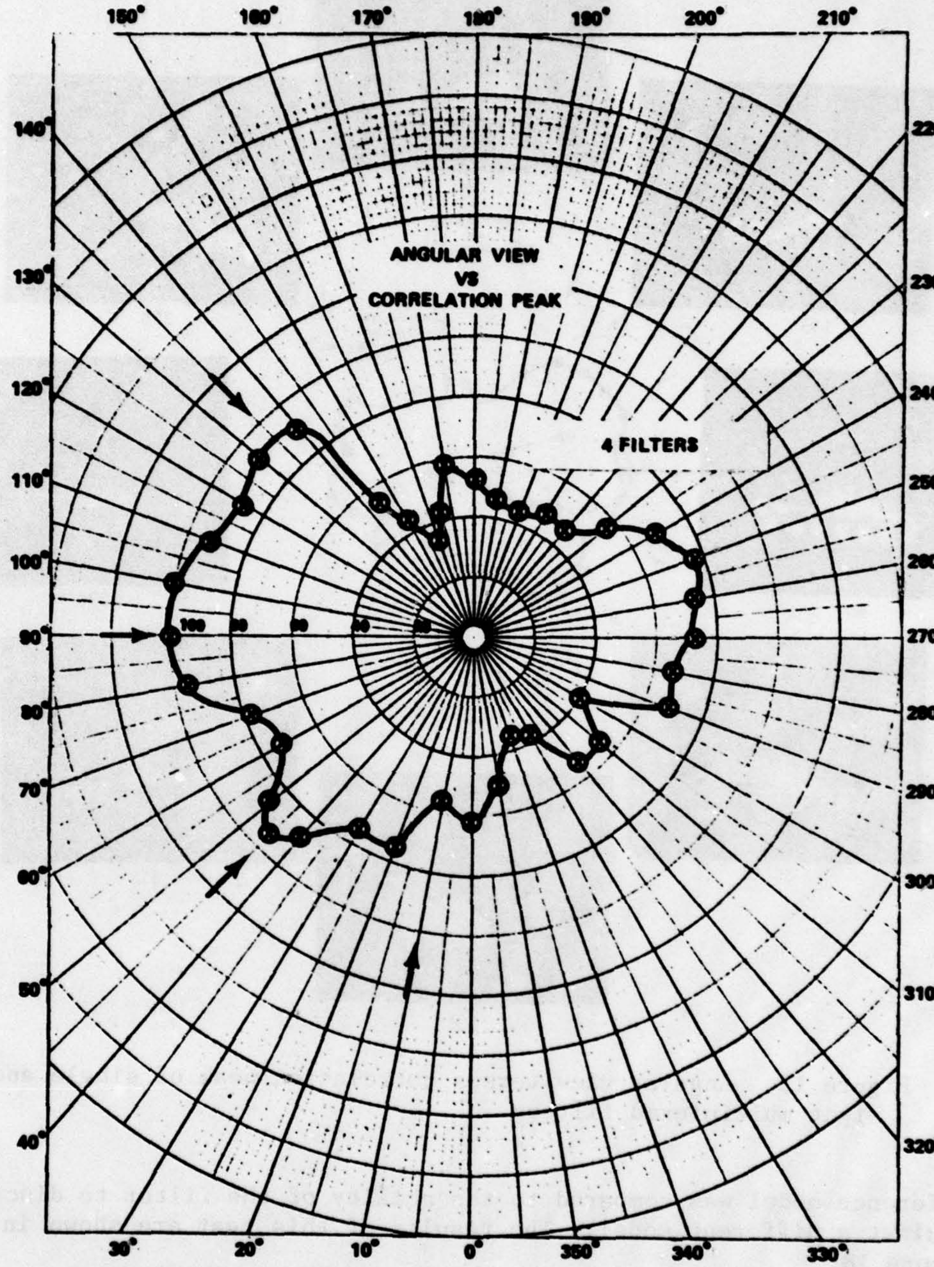

Figure 16. Angular view versus correlation peak of four multiplexed filters.

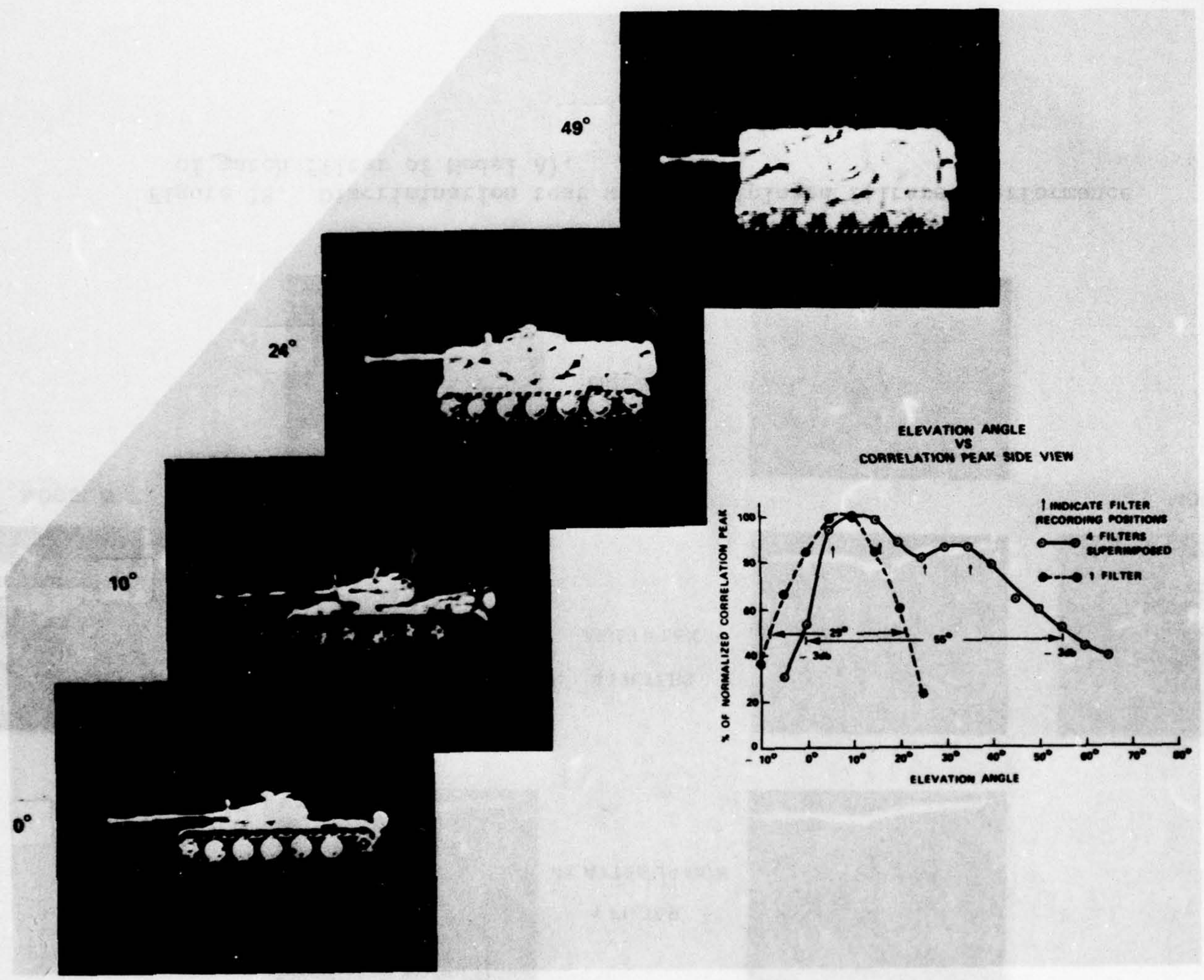

Figure 17. Elevation versus correlation peak of single and multiplexed filters.

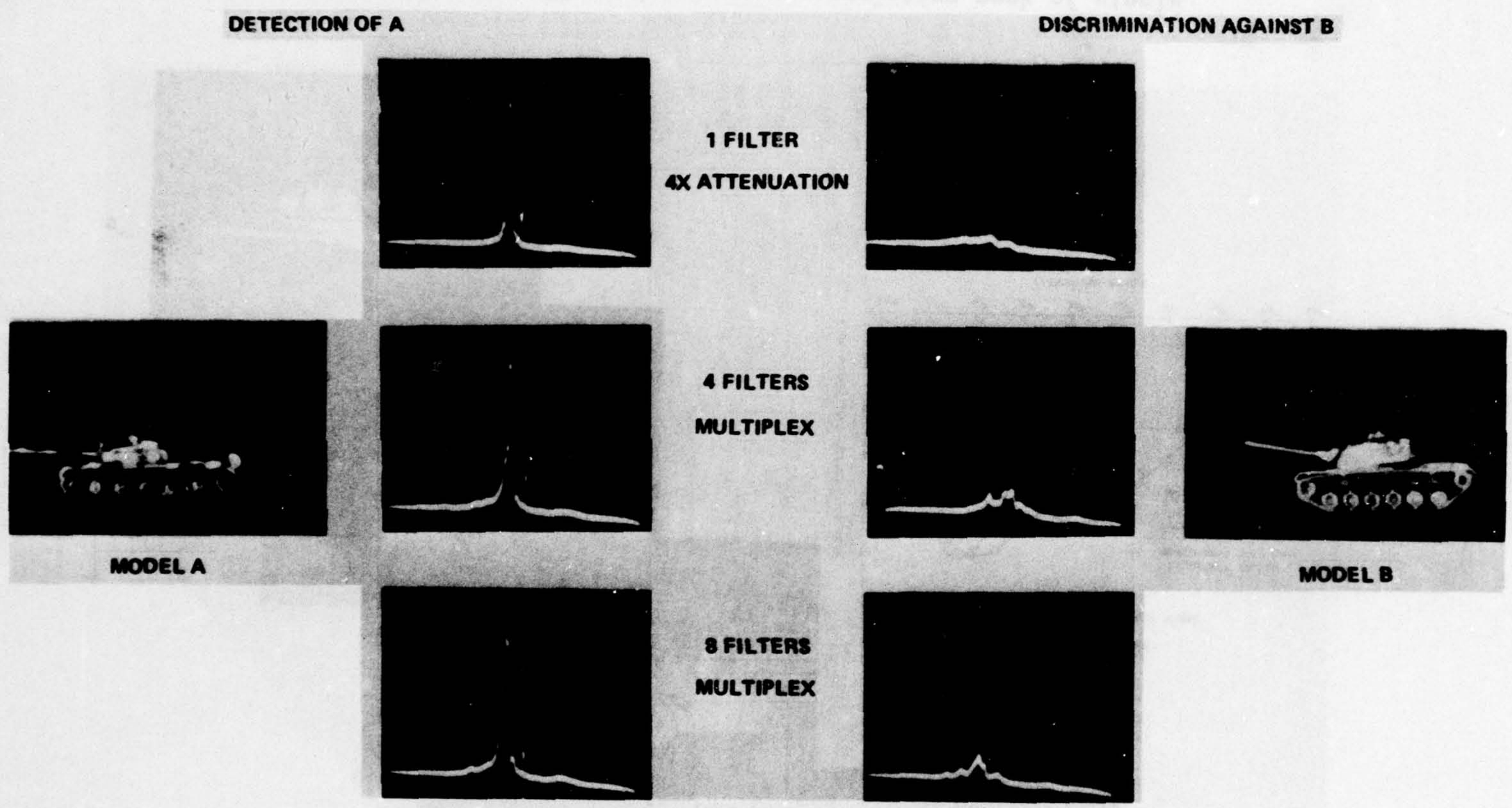

Figure 18. Discrimination test with multiplexed filters (performance of match filter of Model A).

the eight multiplex filters was unexpectedly high: one-fourth the amplitude obtained when using a single filter. From linear recording theory one would expect the correlation peak to drop to $1/N^2$ of that of a single filter if only one filter produces a measurable correlation, or to $1/N$ of that of a single filter if all filters simultaneously form correlation peaks that add in intensity (N here is the number of superimposed filters). Apparently the multiplexed filters do not fit either of the previously mentioned cases. The abnormally large correlation peak amplitude may be the result of nonlinear recording and in-phase amplitude addition of the correlation peaks from individual filters.

IV. FUTURE SYSTEM

A large number of reference images can be stored and rapidly addressed in a correlator using parallel channels and superimposed matched filters. The compact correlator illustrated in Figure 19 is being assembled using components listed in Table 2. To demonstrate the concept four laser diodes, in a 2 × 2 array, will be used as light sources. These diodes can be turned on either sequentially or simultaneously depending on the reference filter arrangement and the correlator application. The cylindrical lenses L_4 are used with each diode to match the beam spread in the plane parallel to the diode junction to the spread in the plane perpendicular to the junction. A TV monitor with relatively low resolution will be used as the input to the liquid crystal light modulator. The image size on the modulator will be approximately 10 mm × 10 mm. Because only low resolution imagery will be used as an input, the resolution limits of the modulator [10] will not be approached. The fact that only low resolution imagery will be used also allows us to reduce the diameter and focal length of the various lenses in the correlator. The correlation peaks from the 2 × 2 matched filter array will be detected by a charge-coupled solid-state detector array with a response matched to the laser diode emission.

V. SUMMARY AND CONCLUSIONS

Several aspects of coherent optical correlators were demonstrated that should make them applicable to a variety of real-world situations. A moving vehicle was tracked in real time over large variations in scale and aspect angles, and the tracking range was increased by using two filters in parallel with a single input image. It was also demonstrated that filter multiplexing can be used to recognize a vehicle from any viewing angle. The relatively low information content enabled the system to operate without liquid gates and allowed a compact correlator to be designed. With the availability of laser diodes and small incoherent-to-coherent image converters, compact optical processors can be constructed that will operate in real time.

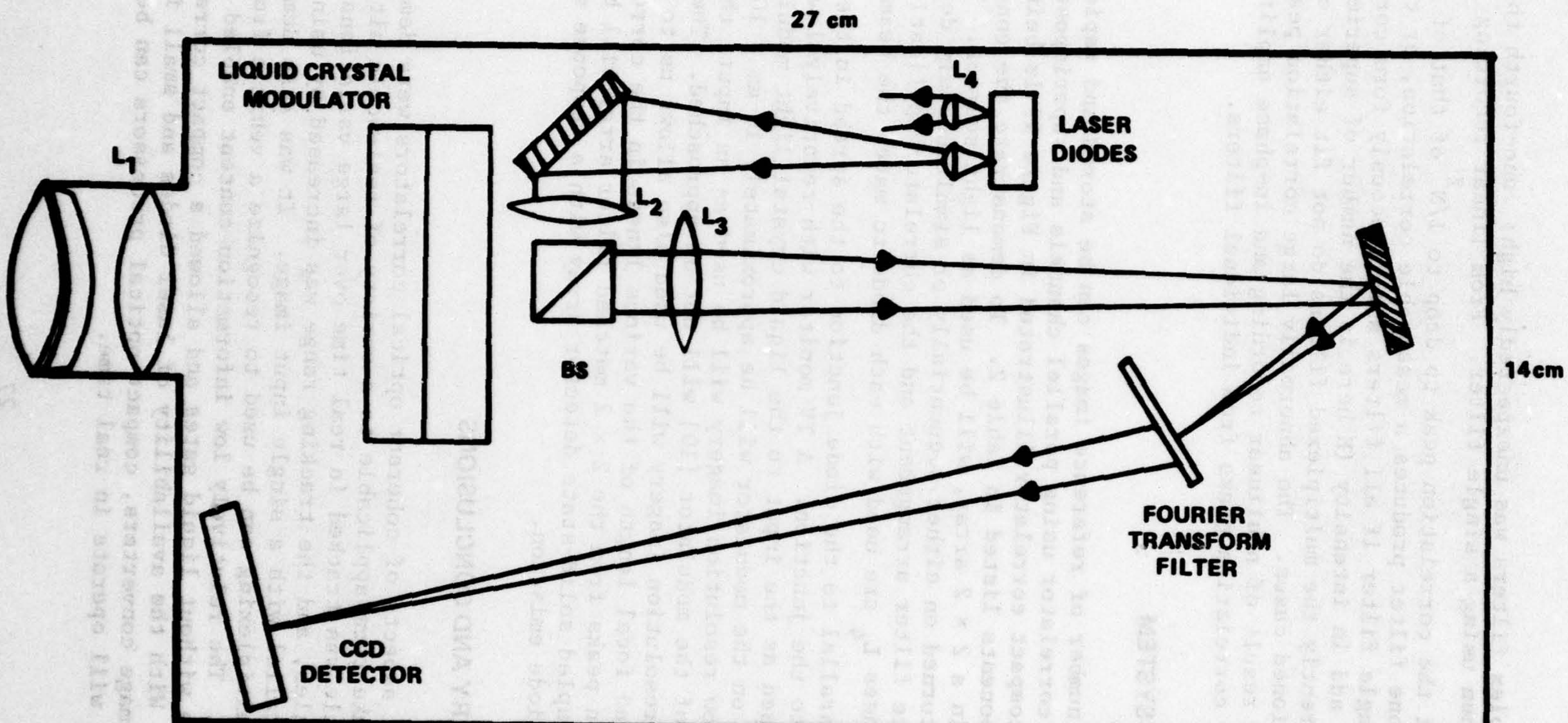

Figure 19. Real-time multichannel coherent optical processor.

TABLE 2. CORRELATOR COMPONENTS

Lenses	Focal Length	Comment
L_1	50 mm	f/1.2 Camera Lens
L_2	100 mm	25-mm Diameter
L_3	200 mm	25-mm Diameter
L_4	7 mm	Cylindrical

NOTE: Liquid Crystal Light Modulator: Hughes Aircraft
Laser Diodes: RCA Type C30130
Detector: RCA Type SID52501
Beam Splitter: 15 × 15 mm polarizing type
Correlator Size: 14 × 27 × 10 cm

The critical elements of a real-time correlator are a fast coherent input image device and near real-time filter recording medium. The Hughes liquid-crystal incoherent-to-coherent imaging device has worked well, but further improvements are necessary. Smaller size, longer life-time, and faster transient response are needed. This device is best suited for situations where a scene is directly imaged onto the converter.

For situations where the input signal is in electronic form, a direct conversion to a coherent image without cathode ray tube (CRT) display and imaging would be desirable. In the present configuration, even a small CRT and an imaging lens would occupy as much space as the complete correlator. Reports of direct electronic signal to coherent image conversion devices have appeared in trade journals and these are presently in experimental stages. Further development of such devices is required.

Photoconductor-thermoplastic materials appear to be best suited for near real-time matched filter construction. The recording cycle is less than 1 sec and is permanent until erased. A commercial unit has appeared on the market but is rather large and not suitable for incorporation into the correlator. The recording device could be very compact if specifically designed for correlator use, and such development is highly desirable.

REFERENCES

1. Guenther, B. D., Christensen, C. R., Greer, M. O., and Rotz, F. B., "Optical Cross-Correlation for Terminal Guidance," Proc. of AIAA Guidance and Control Conference, Stanford California, August 1972.

2. Upatnieks, J., Real-Time Optical Correlator for Missile Guidance, Final Report, Battelle Task No. 0489, November 1977.

3. Leib, K. D. et al., "Aerial Reconnaissance Film Screcning Using Optical Matched-Filter Image-Correlation Technology," Applied Optics, Vol. 17, September 1978, p. 2892.

4. Gara, A. D., "Real Time Optical Correlation of 3-D Scenes," Applied Optics, Vol. 16, January 1977, p. 149.

5. Vander Lugt, A., Rotz, F. B., and Klooster, A., Jr., "Character-Reading by Optical Spatial Filtering," J. T. Tippett (editor), Optical and Electro-Optical Information Processing, Cambridge: MIT Press, 1965, p. 125.

6. Vander Lugt, A., "Coherent Optical Processing," Proc. of IEEE, Vol. 62, 1974, p. 1300.

7. Williams, R. W., von Bieren, K., Moraless, M., "Wide Aperture Optical Correlator-Spectrum Analyzer: Evaluation of a New Design," Applied Optics, Vol. 14, 1975, p. 2944.

8. "Optics in Radar Systems," B. W. Vatz (editor), Proc. of SPIE, Vol. 128, 1977.

9. Grinberg, J., Jacobson, A. J., Bleha, W., Miller, L., Fraas, L., Boswell, D., and Myer, G. "A New Real Time Non-Coherent to Coherent Light Image Converter: The Hybrid Field Effect Liquid Crystal Light Valve," Optical Engineering, Vol. 14, 1975, p. 217.

10. Bleha, W. P., Lipton, L. T., Wiener-Avnear, E., Grinberg, J., Reif, P. G., Casasent, D., Brown, H. B., Markevitch, B. V., "Application of the Liquid Crystal Light Valve to Real Time Optical Data Processing," Optical Engineering, Vol. 17, 1978, p. 371.

11. "Perception of Displayed Information," L. M. Biberman (editor), Plenum Press: New York, 1973.

12. Upatnieks, J., Guenther, B. D., Christensen, C. R., Real-Time Correlation for Missile Terminal Guidance, US Army Missile Research and Development Command, Technical Report H-78-5, January 1978.

DISTRIBUTION

	No. of Copies
Commander Defense Documentation Center Attn: DDC-TCA Cameron Station Alexandria, Virginia 22314	12
Commander US Army Research Office Attn: Dr. R. Lontz P. O. Box 12211 Research Triangle Park, North Carolina 27709	2
US Army Research and Standardization Group (Europe) Attn: DRXSN-E-RX, Dr. Alfred K. Nedoluha Box 65 FPO, New York 09510	2
US Army Material Development and Readiness Command Attn: Dr. Gordon Bushy Dr. James Bender Dr. Edward Sedlak 5001 Eisenhower Avenue Alexandria, Virginia 22333	1 1 1
Headquarters Attn: DA(DAMA-ARZ) Washington, D. C. 20301	2
Under Secretary of Defense for Research and Engineering Attn: Mr. L. Weisberg Washington, D.C. 20301	2
Director Defense Advanced Research Project Agency/STO Attn: Commander T. F. Wiener D. W. Walsh 1400 Wilson Boulevard Arlington, Virginia 22209	1 1
Commander US Army Aviation Systems Command 12th and Spruce Streets St. Louis, Missouri, 63166	1
Director US Army Air Mobility Research and Development Laboratory Ames Research Center Moffett Field, California 94035	1
Commander US Army Electronics Research & Development Command Attn: DRSEL-TL-T, Dr. Jacobs DRSEL-CT, Dr. R. Buser DELEW-E, Henry E. Sonntag Fort Monmouth, New Jersey 07703	1 1 1
Director US Army Night Vision Laboratory Attn: John Johnson Fort Belvoir, Virginia 22060	1
Commander US Army Picatinny Arsenal Dover, New Jersey 07801	1
Commander US Army Harry Diamond Laboratories 2800 Powder Mill Road Adelphi, Maryland 20783	1
Commander US Army Foreign Science and Technology Center Attn: W. S. Alcott Federal Office Building 220 7th Street, NE Charlottesville, Virginia 22901	1
Commander US Army Training and Doctrine Command Fort Monroe, Virginia 22351	1

	No. of Copies
Director Ballistic Missile Defense Advanced Technology Center Attn: ATC-D, R. E. Dace J. M. McKay ATC-O ATC-R, B. Vatz ATC-T P. O. Box 1500 Huntsville, Alabama 35808	1 1 1 1 1
Commander US Naval Air Systems Command Missile Guidance and Control Branch Washington, D. C. 20360	1
Chief of Naval Research Department of the Navy Washington, D. C.	1
Commander US Naval Air Development Center Warminster, Pennsylvania 18974	1
Commander US Naval Ocean Systems Center Attn: Code 7313, T. Medcalf Code 8111, Keith Bromley 271 Catalina Blvd. San Diego, California 92152	1 1
Director Naval Research Laboratory Attn: Dave Ringwolt Code 5570, T. Gialborinzi Washington, D. C. 20390	1 1
Commander Rome Air Development Center US Air Force Attn: James Wasielewski, IRRC Griffiss Air Force Base, New York 13440	1
Commander US Air Force, AFOSR/NE Attn: Dr. J. A. Neff Building 410 Bolling Air Force Base Washington, D. C. 20332	1
Commander US Air Force Avionics Laboratory Attn: D. Rees Dr. E. Champaign Dr. J. Ryles Gale Urban David L. Flannery Wright Patterson Air Force Base, Ohio 45443	1 1 1 1 1
Commander Attn: AFATL/LMT, Charles Warren Eglin Air Force Base, Florida 32544	1
Environmental Research Institute of Michigan Radar and Optics Division Attn: Dr. A. Kozma Dr. C. C. Aleksoff Juris Upatnieks P. O. Box 618 Ann Arbor, Michigan 41807	1 1 1
Physics Department University of Alabama Attn: Dr. J. G. Castle 4701 University Drive, N. W. Huntsville, Alabama 35807	1
Science and Technology Division Institute of Defense Analysis Attn: Dr. Vincent J. Corcoran 400 Army-Navy Drive Arlington, Virginia 22202	1
Optical Science Consultants Attn: Dr. D. L. Fried P. O. Box 446 Placentia, California 92670	1

	No. of Copies
Commander Center for Naval Analyses Attn: Document Control 1401 Wilson Boulevard Arlington, Virginia 22209	1
Raytheon Company Attn: A. V. Jelalian 528 Boston Post Road Sudbury, Maryland 01776	1
Information Systems Laboratory Department of Electrical Engineering Attn: Dr. J. W. Goodman Stanford University Stanford, California 94305	1
National Bureau of Standards Attn: Eric G. Johnson, Jr. 325 S. Broadway Boulder, Colorado 80302	1
Battelle Columbus Labs Attn: M. Vanderlind 505 King Ave. Columbus, Ohio 43201	1
The Institute of Optics University of Rochester Attn: Dr. Nicholas George Rochester, New York 14627	1
Naval Avionics Facility Indianapolis, Indiana 46218	1
Harris Corporation Attn: F. B. Rotz P. O. Box 37 Melbourne, Florida 32901	1
TAI Corporation Attn: Robert L. Kurtz 8302 Whitesburg Dr., S. E. Huntsville, Alabama 35802	1
Itek Corporation Attn: J. R. Vyce 10 Maguire Road Lexington, Massachusetts 02173	1
Carnegie Mellon University Hamerschlag Hall, Room 106 Attn: Dr. David Casasent Pittsburgh, Pennsylvania 15213	1
McDonnell Douglas Astronautics Attn: David M. Karnes 5301 Bolsa Avenue Huntington Beach, California 92647	1
Jet Propulsion Laboratory Building 77 Attn: Paul Shlichta Pasadena, California 91103	1
Westinghouse Electric Corporation Research and Development Center Attn: Gerald B. Brandt Pittsburgh, Pennsylvania 15235	1
Research Department Grumman Aerospace Corporation Attn: E. G. Leib Bethpage, New York 11714	1
Department of Defense Attn: Terry Turpin 9800 Savage Road Ft. George G. Meade, Maryland 20755	1
Electrical Engineering Department Ohio State University Attn: Dr. Stuart A. Collins 1320 Kinnear Road Columbus, Ohio 43212	1

	No. of Copies
Teledyne Brown Engineering Cummings Research Park Attn: Mike Scarborough, MS-19 Huntsville, Alabama 35807	1
Commander AFEL Hanscom Air Force Base, Maryland 01731	1
Hughes Research Laboratories Attn: Dr. Arthur N. Chester	1
Dr. Donald H. Close	1
Dr. Jan Grinberg	1
Dr. Wilfried O. Eckhardt 3011 Malibu Canyon Road Malibu, California 90265	1
U. S. Army Engineering Topographic Laboratory Attn: Alphonse C. Elser Ft. Belvoir, Virginia 22060	1
Aerodyne Research, Inc. Bedford Research Park Attn: H. J. Caulfield Crosby Drive Bedford, Massachusetts 01730	1
Industrial Products Division Hughes Aircraft Company Attn: Dr. William P. Bleha 6155 El Camino Real Carlsbad, California 92008	1
Commandant US Army Air Defense School Attn: ATSA-CD-CS-A, Major Humphrey Fort Bliss, Texas 79916	1
McDonnell Douglas Astronautics Company - East Attn: Dr. Robert G. Wagner St. Louis, Missouri 63166	1
TRW Defense and Space Systems Group Attn: Dr. Peter O. Clark One Space Park Redondo Beach, California 90278	1
General Electric Company Electromagnetic and Acoustics Electronics Laboratory Attn: Milton L. Noble Syracuse, New York 13201	1
Commander Combined Arms Combat Development Activity Attn: ACTA-CI-CIB/Lt. Col. Williamson Ft. Leavenworth, Kansas 66027	1
J. Edgar Hoover FBI Building Attn: Michal Didyk 10 and Pennsylvania Ave., N. W. Washington, D. C. 20535	1
Georgia Institute of Technology School of Electrical Engineering Attn: William Rhodes Atlanta, Georgia 30332	1
United Technologies Research Center Attn: Anthony J. DeMaria E. Hartford, Connecticut 06108	1
Vought Corporation Advanced Technology Center P.O. Box 226144 Attn: Dr. D. D. Eden Dallas, Texas 75266	1
Southern Technologies Attn: G. C. Renfroe 1013 Meridian Street N. Huntsville, Alabama 35801	1

	No. of Copies
DRCPM-PE	1
DRCPM-PE-E	1
DRSMI-LP, Mr. Voigt	1
DRDMI-X, Mr. McKinley	1
-T, Dr. Kobler	1
James Fagan	1
-H, Dr. J. P. Hallowes, Jr.	1
-HS, Jerry Hagood	2
-TE, W. Pittman	1
R. Russell	1
C. E. Kulas	1
L. G. Minor	1
-TG	1
-TG, J. A. McLean	1
-TB	1
-C	1
-Y	1
-TR, Dr. R. L. Hartman	1
Dr. J. S. Bennett	1
Dr. C. R. Christensen	80
Dr. B. D. Guenther	1
Dr. J. L. Smith	1
Dr. J. D. Stettler	1
-TBD	3
-TI (Record Set)	1
(Reference Copy)	1